Computational Physics Final Project
1D MHD code building and testing

Xu-Yao Hu
Department of Physics, New York University

December 16, 2016

Abstract

A one-dimensional MHD code using PLM + HLLD is constructed. Compared to the code with the regular HLL scheme, the code based on HLLD is confirmed to be less diffusive, which indicates that HLLD scheme is more advanced and more suitable to be applied in MHD code. Several shock tube tests, rarefaction wave tests are performed to examine the effectiveness and the accuracy of my MHD code. The results given by my MHD code agree with those presented in previous papers. A sinusoidal Alfvén wave example is constructed using my MHD code. The wave speed of the constructed Alfvén wave obtained using my MHD code is consistent with the theoretical expectation. An animation of Alfvén Wave is generated, which presents a more clear scenario of this dynamical process.

1 Introduction

Magnetohydrodynamics (MHD) is extremely important in various fields such as Astrophysics, Geophysics and Plasma Physics.

The thrust of this work is to construct a reliable 1D MHD code by using higher-order Piecewise Linear Method (PLM) and Harten-Lax-van Leer (HLL) type Riemann Solvers. We attempt to construct both PLM + regular HLL code and PLM + HLLD code, and run several test problems to check the effectiveness and the accuracy of the code.

For an ideal MHD system, the basic dynamics equations are the mass conservation equation, the momentum conservation equation, the energy conservation equation, and Ohm's law with Maxwell's Equations. All equations can be written in conservative form as (See [4])

$$\frac{\partial \rho}{\partial t} + \boldsymbol{\nabla} \cdot (\rho \boldsymbol{v}) = 0 \ , \tag{1}$$

$$\frac{\partial \rho \boldsymbol{v}}{\partial t} + \boldsymbol{\nabla} \cdot (\rho \boldsymbol{v}\boldsymbol{v} - \boldsymbol{B}\boldsymbol{B} + \boldsymbol{P}_T) = 0 \ , \tag{2}$$

$$\frac{\partial E}{\partial t} + \boldsymbol{\nabla} \cdot [(E + P_T)\boldsymbol{v} - \boldsymbol{B}(\boldsymbol{B} \cdot \boldsymbol{v})] = 0 \ , \tag{3}$$

$$\frac{\partial \boldsymbol{B}}{\partial t} - \boldsymbol{\nabla} \times (\boldsymbol{v} \times \boldsymbol{B}) = 0 \ . \tag{4}$$

where ρ is the fluid mass density, $\boldsymbol{v} = (v_x, v_y, v_z)$ is the flow velocity, $\boldsymbol{B}$ is the magnetic field, E is the total energy density, $\boldsymbol{P}_T \equiv P_T \boldsymbol{I}$ is a diagonal tensor with components $P_T = P + \frac{1}{2}B^2$ with P being the pressure. The equations above are written in units such that the magnetic permeability $\mu = 1$. To close the equations, we usually need the

equation of state (EoS) for ideal fluid (gas). Actually, EoS can be encoded in the expression of the total energy density

$$E = \frac{P}{\gamma - 1} + \frac{1}{2}\rho v^2 + \frac{B^2}{2} \ , \tag{5}$$

where γ is the adiabatic index of the ideal gas. It is useful to write down the explicit form of the thermodynamical pressure

$$P = (\gamma - 1)\left[E - \frac{1}{2}\rho v^2 - \frac{B^2}{2}\right] \ . \tag{6}$$

2 Numerical Method

2.1 1D MHD in Cartesian coordinates

The project starts with solving 1D effective problems (all physical quantities depend on one position component, say x, and time t). The 1D MHD equations can be cast into a compact form as

$$\frac{\partial \boldsymbol{U}}{\partial t} + \frac{\partial \boldsymbol{F}}{\partial x} = 0 \ , \tag{7}$$

where $\boldsymbol{U}$ and $\boldsymbol{F}$ are the vectors of all conserved variables and fluxes in Cartesian coordinates respectively and given by $\boldsymbol{U} = (\rho, \rho v_x, \rho v_y, \rho v_z, E, B_x, B_y, B_z)^T$ and $\boldsymbol{F} = (\rho v_x, \rho v_x^2 + P_T - B_x^2, \rho v_x v_y - B_x B_y, \rho v_x v_z - B_x B_z, (E + P_T)v_x - (\boldsymbol{B}\cdot\boldsymbol{v})B_x, 0, B_y v_x - B_x v_y, B_z v_x - B_x v_z)^T$. Since the sixth pair of components are trivial in 1D case (B_x = constant), we use the simplified form of the vectors for 1D code as follows,

$$\boldsymbol{U} = \begin{pmatrix} \rho \\ \rho v_x \\ \rho v_y \\ \rho v_z \\ E \\ B_y \\ B_z \end{pmatrix} \ , \qquad \boldsymbol{F} = \begin{pmatrix} \rho v_x \\ \rho v_x^2 + P_T - B_x^2 \\ \rho v_x v_y - B_x B_y \\ \rho v_x v_z - B_x B_z \\ (E + P_T)v_x - (\boldsymbol{B}\cdot\boldsymbol{v})B_x \\ B_y v_x - B_x v_y \\ B_z v_x - B_x v_z \end{pmatrix} \ . \tag{8}$$

It is often useful to introduce the vector of primitive variables:

$$\boldsymbol{Q} = \begin{pmatrix} \rho \\ v_x \\ v_y \\ v_z \\ P \\ B_y \\ B_z \end{pmatrix} \ . \tag{9}$$

2.2 Algorithm

The algorithm of my 1D MHD code is described in details in this section.

Step 1 Input the initial conditions of the MHD system and write them in terms of the conserved variable vector $\boldsymbol{U}$ and the fluxes vector $\boldsymbol{F}$.

Step 2 Construct the "left" and "right" states at every interface using Piecewise Linear Method (PLM) [This part is done by `PLM` function in `MHD_1d_Solver_Scheme.py`.]

(a) Receive $\boldsymbol{U}$ vector (for each cell center) and convert it into $\boldsymbol{Q}$ vector (for each cell center);
Technicall details: Both $\boldsymbol{U}$ and $\boldsymbol{Q}$ are $7 \times (N+4)$ matrices with $i = 2, 3, \cdots N+1$ representing real cells (N real cells in total) and $i = 0, 1, N+2, N+3$ denoting ghost cells.

(b) Using PLM to get $\boldsymbol{Q}_L$ (for each interface) and $\boldsymbol{Q}_R$ (for each interface) from $\mathbf{Q}$ (for each cell center);
Technical details: To make things easy to track, we also set $\boldsymbol{Q}_L$ and $\boldsymbol{Q}_R$ as $7 \times (N+4)$ matrices with $i = 1, 2, \cdots, N+1$ are real interfaces that we're interested in and $i = 0, N+2, N+3$ being spare interfaces on which no operation is performed. By "real" interfaces, I refer to the interfaces which are the boundaries of the real cells.

(c) Calculate the fast magneto-acoustic wave speeds for the "left" and "right" states, i.e. c_{fL} and c_{fR} using the following equation:

$$c_f = \left[\frac{\gamma P + |\boldsymbol{B}|^2 + \sqrt{(\gamma P + |\boldsymbol{B}|^2)^2 - 4\gamma P B_x^2}}{2\rho} \right]^{1/2} , \tag{10}$$

thus obtaining the smallest and the largest eigenvalues $\lambda_1 = v_x - c_f$ and $\lambda_7 = v_x + c_f$ for the "left" and "right" states.

(d) Determine the minimum and maximum signal speed as

$$S_L = \min[\lambda_1(\boldsymbol{U}_L), \lambda_1(\boldsymbol{U}_R)] , \tag{11}$$

$$S_R = \max[\lambda_7(\boldsymbol{U}_L), \lambda_7(\boldsymbol{U}_R)] . \tag{12}$$

Step 3 Compute the flux at each real interface using a HLL-type Riemann Solver[1] (This part is done by functions `F_HLL_generator` and `F_HLLD_generator` in `MHD_1d_Solver_Scheme.py`)

- For HLL Solver:
  Calculate the intermediate fluxes $\boldsymbol{F}^*$ and the HLL fluxes is given by

$$\boldsymbol{F}_{\rm HLL} = \begin{cases} \boldsymbol{F}_{\rm L} & \text{if } S_L > 0 , \\ \boldsymbol{F}^* & \text{if } S_L \le 0 \le S_R , \\ \boldsymbol{F}_{\rm R} & \text{if } S_R < 0 . \end{cases} \tag{13}$$

- For HLLD Solver:
  Calculate the intermediate fluxes $\boldsymbol{F}_L^*$, $\boldsymbol{F}_L^{**}$, $\boldsymbol{F}_R^*$, $\boldsymbol{F}_R^{**}$ and the HLLD fluxes is given by

$$\boldsymbol{F}_{\rm HLLD} = \begin{cases} \boldsymbol{F}_{\rm L} & \text{if } S_L > 0 , \\ \boldsymbol{F}_{\rm L}^* & \text{if } S_L \le 0 \le S_L^* , \\ \boldsymbol{F}_{\rm L}^{**} & \text{if } S_L^* \le 0 \le S_M , \\ \boldsymbol{F}_{\rm R}^{**} & \text{if } S_M \le 0 \le S_R^* , \\ \boldsymbol{F}_{\rm R}^* & \text{if } S_R^* \le 0 \le S_R , \\ \boldsymbol{F}_{\rm R} & \text{if } S_R < 0 . \end{cases} \tag{14}$$

[1] For more details about HLL and HLLD, see Mitoshi & Kusano [3]

Step 4 Update the cell-centered conserved variables using the third-order Runge-Kutta scheme devised by Shu & Osher:

$$\mathbf{U}^{(1)} = \mathbf{U} + \Delta t L(\mathbf{U}^n) \ , \tag{15}$$

$$\mathbf{U}^{(2)} = \frac{3}{4}\mathbf{U}^n + \frac{1}{4}\mathbf{U}^{(1)} + \frac{1}{4}\Delta t L(\mathbf{U}^{(1)}) \ , \tag{16}$$

$$\mathbf{U}^{n+1} = \frac{1}{3}\mathbf{U}^n + \frac{2}{3}\mathbf{U}^{(2)} + \frac{2}{3}\Delta t L(\mathbf{U}^{(2)}) \ , \tag{17}$$

where $L(\boldsymbol{U_i}) = -\frac{\boldsymbol{F}_{\mathrm{HLLD},i+1/2} - \boldsymbol{F}_{\mathrm{HLLD},i-1/2}}{\Delta x}$ for HLLD fluxes and Δt is determined by CFL stability condition

$$\Delta t = C_{\mathrm{CFL}} \Delta x / \max(v^n_{x,i} + c^n_{f,i}) \ , \tag{18}$$

where $C_{\mathrm{CFL}} < 1$ is referred to as CFL number.

3 Numerical Tests

All relevant numerical test results and discussions of my 1d MHD code are elaborated in this section.

3.1 Dai & Woodward shock tube test

Dai & Woodward (1994) [1] proposed a typical one-dimensional shock tube problem, which was solved by Miyoshi & Kusano [3] in the interval $x \in [-0.5, 0.5]$ with 800 cells and CFL number 0.8. The initial conditions ($t = 0$) are given by

$$(\rho,\ P,\ v_x,\ v_y,\ v_z,\ B_y,\ B_z) = (1.08, 0.95, 1.2, 0.01, 0.5, 3.6/\sqrt{4\pi}, 2/\sqrt{4\pi}) \quad \text{for } x < 0 \ , \tag{19}$$

$$(\rho,\ P,\ v_x,\ v_y,\ v_z,\ B_y,\ B_z) = (1, 1, 0, 0, 0, 4/\sqrt{4\pi}, 2/\sqrt{4\pi}) \quad \text{for } x > 0 \ , \tag{20}$$

with $B_x = 4/\sqrt{4\pi}$. The exact solution of this shock tube problem includes several shocks and discontinuities: two fast shocks, two rotational discontinuities, two slow shocks, and a contact discontinuity.

Fig. 1 shows the distribution of all physical quantities at time $t = 0.2$. The zoomed-in graphs confirms the statement that the regular HLL scheme is more diffusive than the HLLD scheme. My code indeed captures all the features of Dai & Woodward shock as did by Miyoshi & Kusano [3].

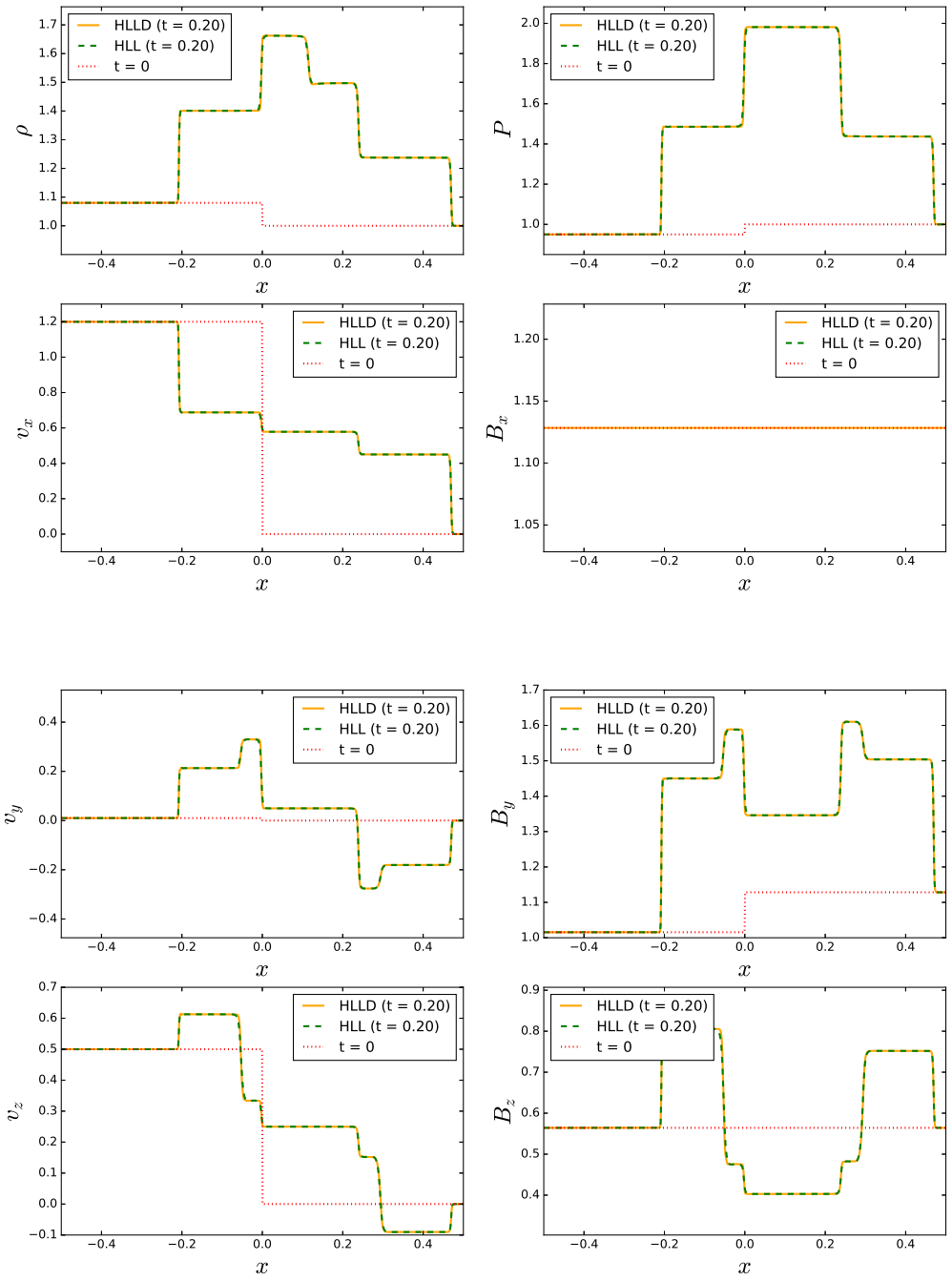

Figure 1: Numerical solutions of Dai & Woodward shock tube at time $t = 0.2$ using HLLD and HLL schemes are plotted. The red dotted curves are the initial conditions of the shock tube.

3.2 Brio & Wu test

A standard test for MHD code is Brio & Wu test. Following Stone et al. (2008) [4], the Brio & Wu problem is solved within the region $x \in [0, 1]$ with 800 cells and the initial set-up (at $t = 0$) is given by

$$(\rho,\ P,\ v_x,\ v_y,\ v_z,\ B_y,\ B_z) = (1.0, 1.0, 0, 0, 0, 1.0, 0) \quad \text{for } x < 0.5 \ , \tag{21}$$

$$(\rho,\ P,\ v_x,\ v_y,\ v_z,\ B_y,\ B_z) = (0.125, 0.1, 0, 0, 0, -1.0, 0) \quad \text{for } x \geq 0.5 \ , \tag{22}$$

with $B_x = 0.75$ and $\gamma = 2.0$. The CFL number is set to be 0.3.

Fig. 2 illustrates the numerical solution to Brio & Wu shock test at time $t = 0.08$. Compared to the results in previous work (e.g. Stone et al [4] and Miyoshi & Kusano [3]), my MHD code captures all the features of the shocks and discontinuities. However, we should expect more obvious difference between the HLLD realization and the regular HLL realization. The HLLD scheme is supposed to have much higher resolution than the regular HLL scheme since more intermediate states are used in HLLD to accurately depict the fluxes through each interface. This may indicate that my HLLD code could be further promoted to a higher-accuracy version.

3.3 Alfvén Wave realization

To realize a sinusoidal Alfvén wave, we apply PLM + HLLD scheme to study the MHD system with $\gamma = 5/3$ using 800 cells within $x \in [-1, 1]$ and set a periodic boundary for the system. The CFL number is chosen to be 0.6. The initial conditions for the system is given by

$$(\rho,\ P,\ v_x) = (1.0, 1.0, 0) \ , \tag{23}$$

$$(\ v_y,\ v_z) = (0.1 \sin[2\pi x \cos(\alpha)], 0.1 \cos[2\pi x \cos(\alpha)]) \ , \tag{24}$$

$$(B_y,\ B_z) = (0.1 \sin[2\pi x \cos(\alpha)], 0.1 \cos[2\pi x \cos(\alpha)]) \ , \tag{25}$$

with $\alpha = 0$, $B_x = 1.0$. The wave speed of Alfvén wave can be immediately calculated as $c_a = \frac{|B_x|}{\sqrt{\rho}} = 1.0$. By equation (24) and (25), we obtain the wavelength is $\lambda_a = 1$, therefore the period of the Alfvén wave is simply $T_a = \lambda_a / c_a = 1$.

Fig. 3 displays the evolution of the system. The wave shown is a transverse wave with the polarization in $y - z$ plane and the transmission in x direction. The period of the wave constructed is consistent with the theoretical expectation of the Alfvén wave under the given initial conditions.

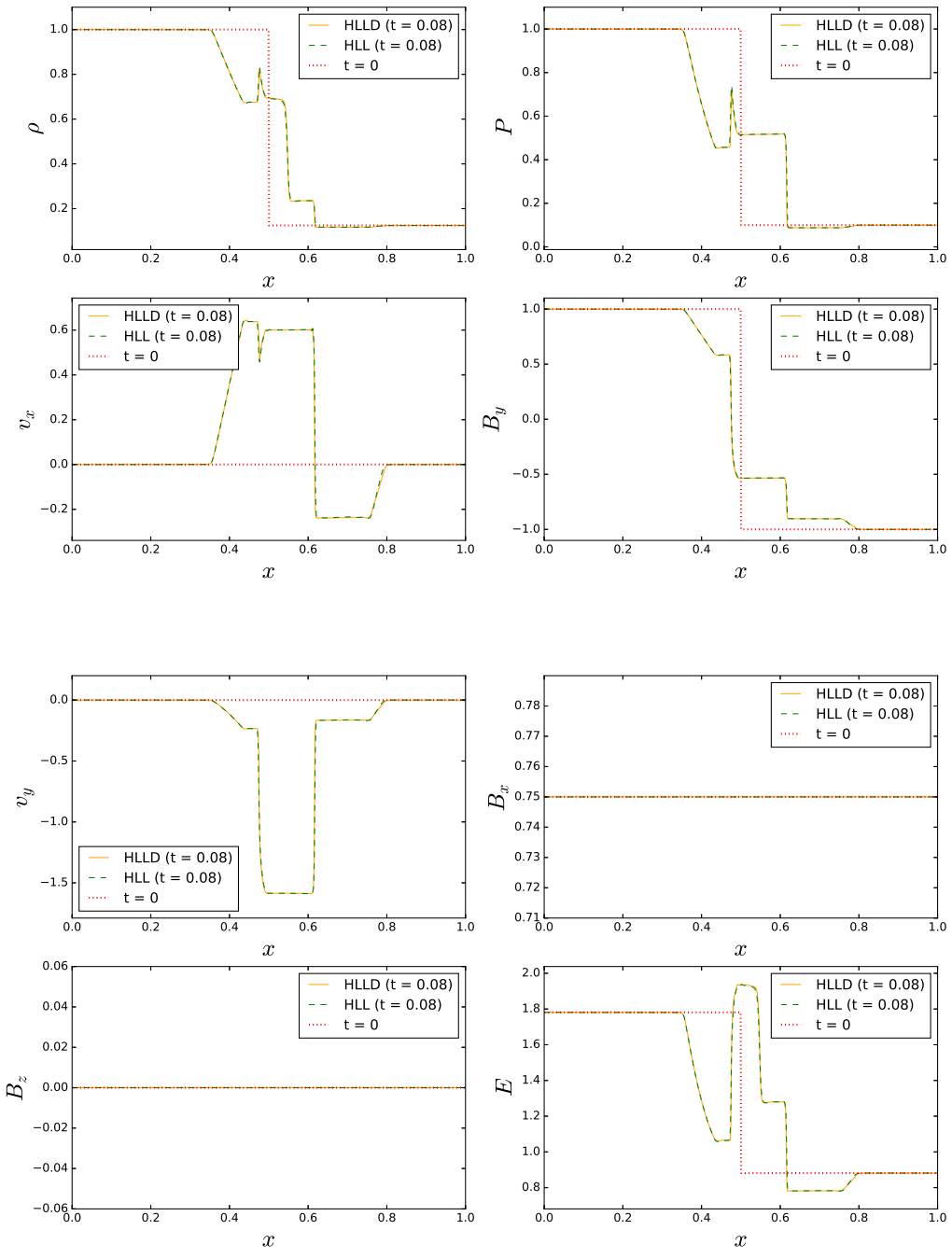

Figure 2: Numerical solutions of Brio & Wu shock test at time $t = 0.08$ using HLLD and HLL schemes are plotted. The red dotted curves are the initial conditions of the shock tube.

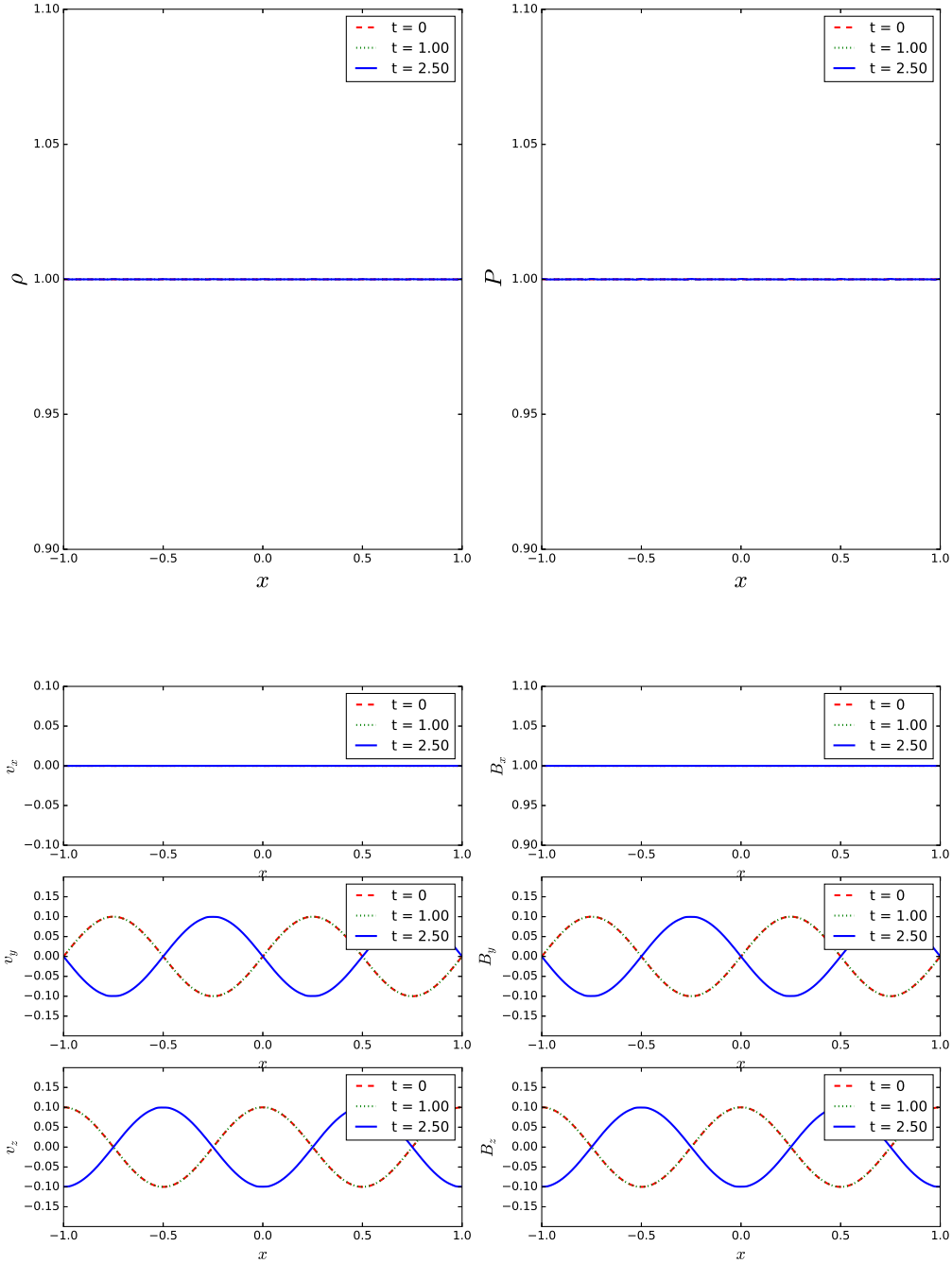

Figure 3: Numerical construction of the Alfvén wave using HLLD scheme is plotted. The red dashed curves are the initial conditions.

3.4 Fast Switch-on (FS) shock

Falle et al. (1998) [2] proposed that the most rational procedure is to test MHD code with a complete set of pure waves rather than compound waves like the shocks in Brio & Wu test. A first example of these pure wave tests is fast switch-on (FS) shock. The FS shock is constructed using PLM + HLLD in the region $x \in [-0.5, 3]$ with 400 cells, $\gamma = 5/3$ and CFL number 0.3. The initial condition is given by

$$(\rho,\ P,\ v_x,\ v_y,\ v_z,\ B_y,\ B_z) = (3, 16.33, -0.732, -1.333, 0, 2.309, 1) \quad \text{for the left half region ,} \tag{26}$$

$$(\rho,\ P,\ v_x,\ v_y,\ v_z,\ B_y,\ B_z) = (1, 1, -4.196, 0, 0, 0, 0) \quad \text{for the right half region ,} \tag{27}$$

with $B_x = 3$ everywhere.

Fig. 4 illustrates the FS shock evolution. Some small-amplitude waves emerge in Fig. 4, which travel away from the shock. It is said that these are generated when the initially discontinuity evolves into a steadily propagating shock with finite width.

3.5 Slow Switch-off (SS) shock

Similarly, Falle et al. proposed the Slow Switch-off (SS) shock test in contrast to FS shock. The SS shock is constructed using PLM + HLLD in the region $x \in [-0.5, 1.5]$ with 400 cells, $\gamma = 5/3$ and CFL number 0.3. The initial condition is given by

$$(\rho,\ P,\ v_x,\ v_y,\ v_z,\ B_y,\ B_z) = (1.368, 1.769, 0.269, 1.0, 0, 0, 0) \quad \text{for the left half region ,} \tag{28}$$

$$(\rho,\ P,\ v_x,\ v_y,\ v_z,\ B_y,\ B_z) = (1, 1, 0, 0, 0, 1, 0) \quad \text{for the right half region ,} \tag{29}$$

with $B_x = 1$ everywhere. Fig. 5 illustrates the SS shock evolution.

3.6 Fast switch-off Rarefaction (FR) wave

Falle et al.[2] also proposed a test in which the initial discontinuity evolves into a fast rarefaction (FR) wave. The FR wave is constructed using PLM + HLLD in the region $x \in [-0.5, 1.5]$ with 400 cells, $\gamma = 5/3$ and CFL number 0.3. The initial condition is given by

$$(\rho,\ P,\ v_x,\ v_y,\ v_z,\ B_y,\ B_z) = (1, 2, 0, 0, 0, 3, 0) \quad \text{for the left half region ,} \tag{30}$$

$$(\rho,\ P,\ v_x,\ v_y,\ v_z,\ B_y,\ B_z) = (0.2641, 0.2175, 3.6, -2.551, 0, 0, 0) \quad \text{for the right half region ,} \tag{31}$$

with $B_x = 1$ everywhere. Fig. 6 shows the FR wave evolution.

3.7 Slow switch-on Rarefaction (SR) wave

In contrast to FR waves, Falle et al.[2] presents a scenario in which an initial discontinuity evolves into a slow rarefaction (SR) wave. The FR wave is constructed using PLM + HLLD in the region $x \in [-0.5, 1.5]$ with 400 cells, $\gamma = 5/3$ and CFL number 0.3. The initial condition is given by

$$(\rho,\ P,\ v_x,\ v_y,\ v_z,\ B_y,\ B_z) = (1, 2, 0, 0, 0, 0, 0) \quad \text{for the left half region ,} \tag{32}$$

$$(\rho,\ P,\ v_x,\ v_y,\ v_z,\ B_y,\ B_z) = (0.2, 0.1368, 1.186, 2.967, 0, 1.6405, 0) \quad \text{for the right half region ,} \tag{33}$$

with $B_x = 1$ everywhere. Fig. 7 shows the SR wave evolution.

4 Conclusions

My one-dimensional MHD code using PLM + HLL/HLLD scheme is able to capture all features of an effective 1D Cartesian MHD system though further promotion is still possible. It successfully passes all kinds of shock wave and rarefaction wave tests mentioned in this work and gives the results similar to those presented in previous papers.

A sinusoidal Alfvén wave is constructed and the wave speed of the wave agrees perfectly with the theoretical expectation.

For future work, we may check the code carefully to find out a way to promote the accuracy of the PLM + HLLD code. Besides, it is interesting to promote this 1D Cartesian code to a 1D cylindrical code (in which all physical quantities depend only on the radius r), which may be useful for modeling an astrophysical disk and studying its dynamics.

The code would be more useful for real MHD system simulation if we promote it to a 3D code like *ATHENA* code [4].

References

[1] Wenlong Dai and Paul R Woodward. An approximate riemann solver for ideal magnetohydrodynamics. *Journal of Computational Physics*, 111(2):354–372, 1994.

[2] SAEG Falle, SS Komissarov, and P Joarder. A multidimensional upwind scheme for magnetohydrodynamics. *Monthly Notices of the Royal Astronomical Society*, 297(1):265–277, 1998.

[3] Takahiro Miyoshi and Kanya Kusano. A multi-state hll approximate riemann solver for ideal magnetohydrodynamics. *Journal of Computational Physics*, 208(1):315–344, 2005.

[4] James M Stone, Thomas A Gardiner, Peter Teuben, John F Hawley, and Jacob B Simon. Athena: a new code for astrophysical mhd. *The Astrophysical Journal Supplement Series*, 178(1):137, 2008.

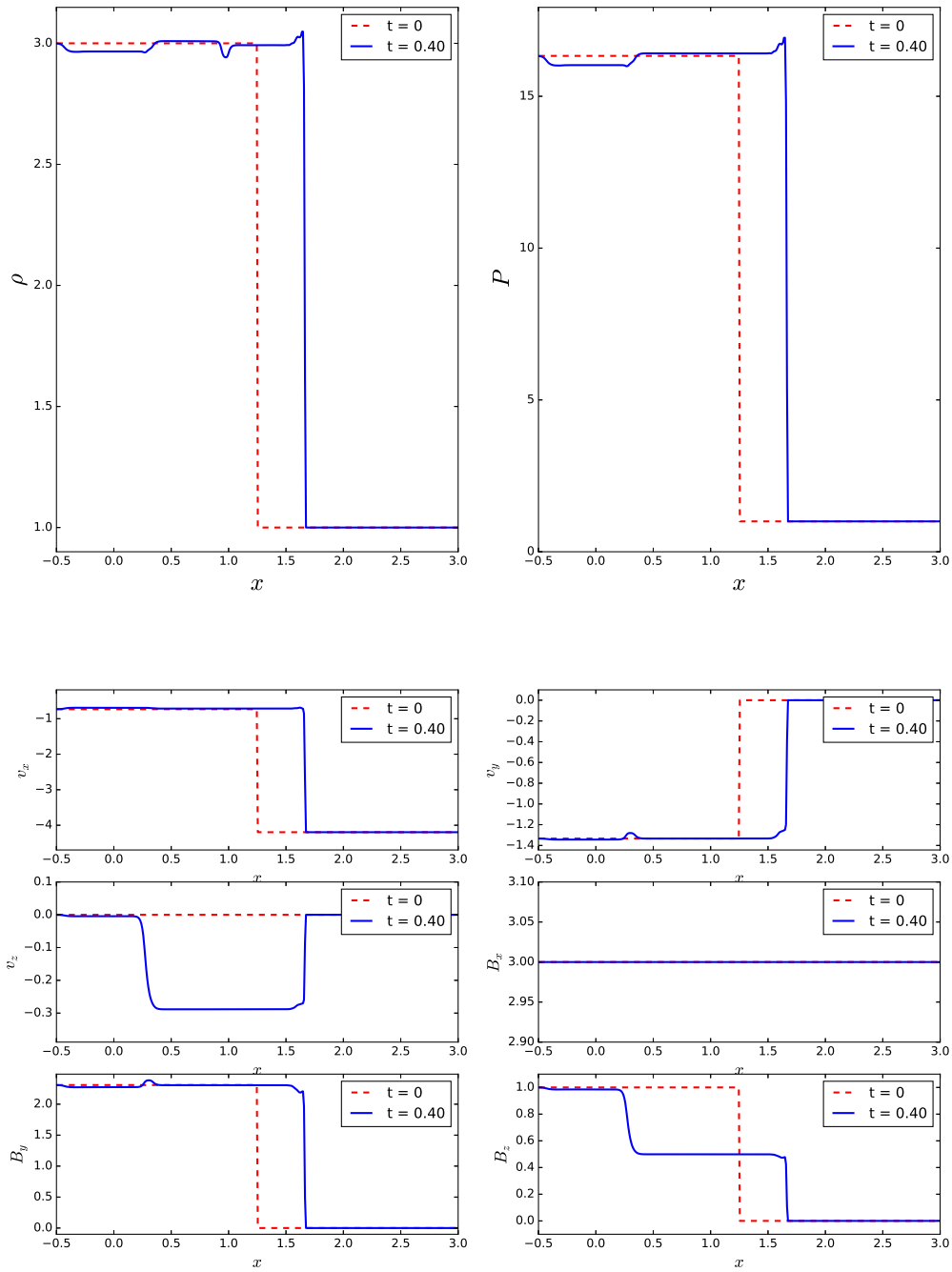

Figure 4: The evolution of FS shock from $t = 0$ to $t = 0.4$ is plotted. The red dashed curves are the initial conditions of the shock tube.

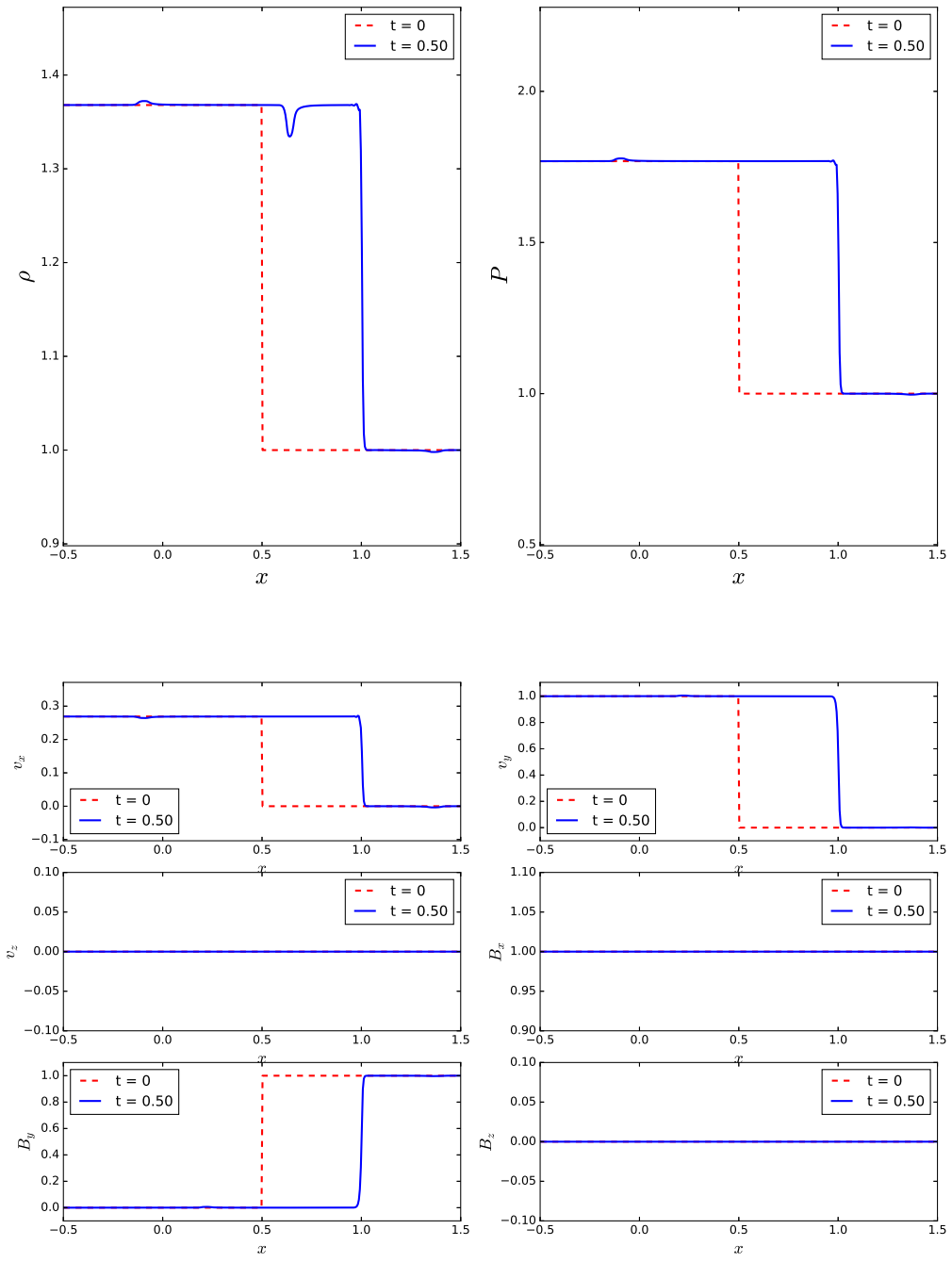

Figure 5: The evolution of SS shock from $t = 0$ to $t = 0.5$ is plotted. The red dashed curves are the initial conditions of the shock tube.

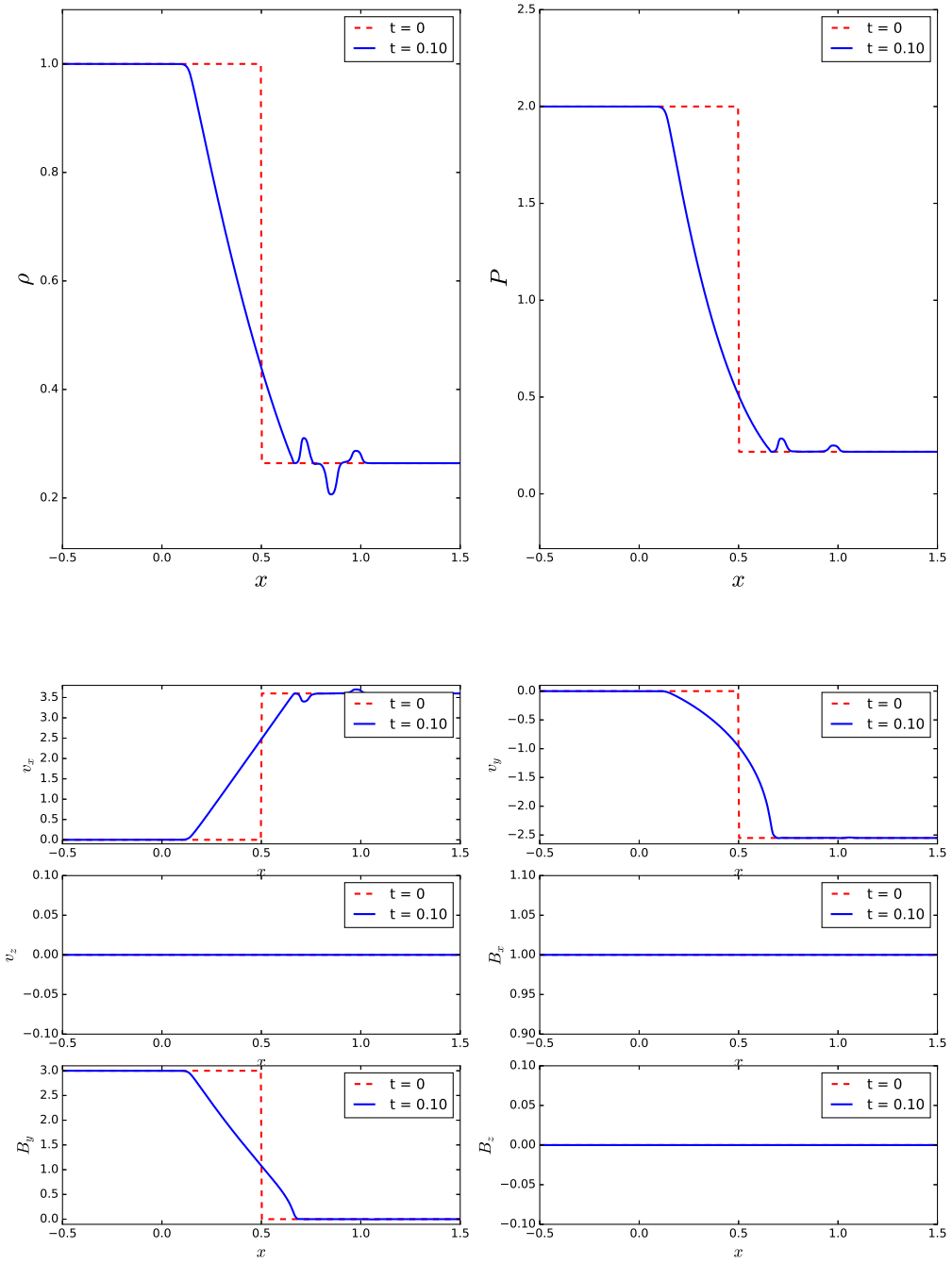

Figure 6: The evolution of FR wave from $t = 0$ to $t = 0.1$ is plotted. The red dashed curves are the initial conditions.

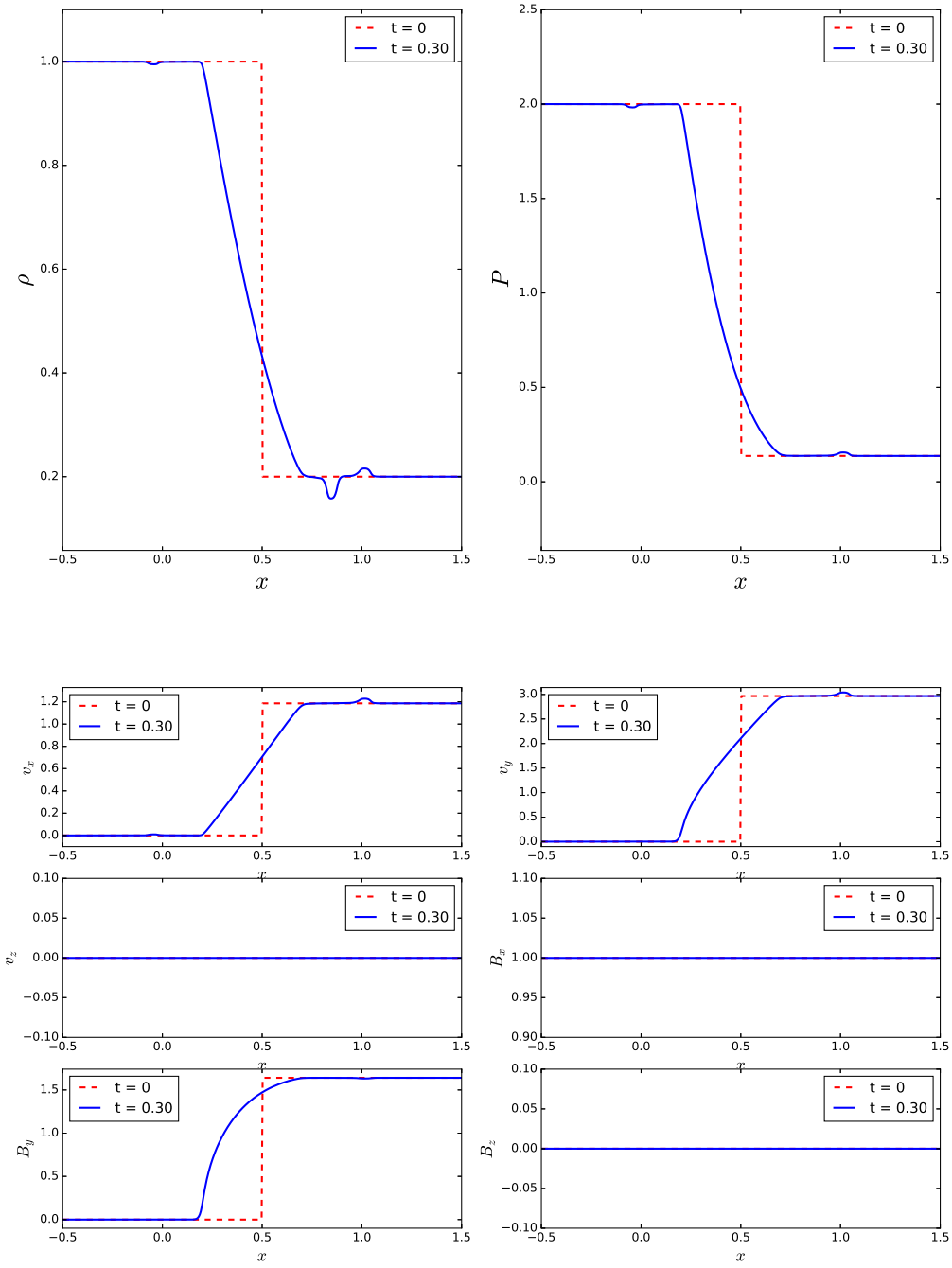

Figure 7: The evolution of SR wave from $t = 0$ to $t = 0.3$ is plotted. The red dashed curves are the initial conditions.